Regularized ICI Cancellation in V2V Communications

E. Vlachos, C. Mavrokefalidis, D. Ampeliotis and K. Berberidis
Computer Engineering and Informatics Dept.
University of Patras, Greece
{vlaxose,maurokef,ampeliot,berberid}@ceid.upatras.gr

ABSTRACT

In this work, we consider a V2V commnunication system operating over high relative speeds. In this scenario, the wireless channel is characterized by double selectivity, which results into intercarrier interference (ICI) at the receiver. To mitigate this effect, several equalization schemes have been proposed, which usually adopt a banded approximation of the frequency domain matrix, in order to reduce the complexity cost. However, these approximations also decrease significantly the performance of the equalizer. To recover this performance loss, we propose a regularized estimation framework for ICI cancellation. The performance superiority of the proposed method against existing ones is verified through extensive simulations which were performed in accordance with the IEEE 802.11p standard. It must be stressed that this improved performance is achieved without increasing the required computational complexity.

CCS Concepts

•**Networks** → **Mobile networks;** *Physical links;* Network algorithms;

Keywords

Vehicle-to-vehicle (V2V); intercarrier interference (ICI); orthogonal frequency division multiplexing (OFDM) communications; banded equalizers; regularization

1. INTRODUCTION

Modern wireless communication systems are expected to support a diverse range of services and requirements that are desired by end-users. The vision of the fifth generation of wireless communications targets data rates in the order of several Gbps, latencies in the order of ms and million of devices interacting to each other in a robust manner [1]. Moreover, mobility requirements are expected to increase in order to cover high-speed scenarios (at least around 250 km/h), while supporting the above specifications. Related applications are, for example, broadcasting of digital audio and digital video [2, 3], mobile radio communications [4, 5], public protection and disaster relief [6].

An active area of research, inherently connected to high-speed scenarios, is vehicular communications [7]. The interaction between vehicles (V2V) and between vehicles and infrastructure nodes (V2I) is the main concern. Target applications and services are for automatic road trafficing, collision avoidance etc. apart from the more classical ones such as communicating and accessing internet [8]. Moreover, several standardization bodies have related activities such IEEE and the associated IEEE 802.11p standard [9].

Orthogonal frequency-division multiplexing (OFDM) has been the main choice for the physical access of the wireless channel considering among others the above applications [2, 3, 4, 5, 9]. In OFDM, the serial data stream is converted into parallel substreams (OFDM blocks) transmitted over narrowband subchannels, which are generally known as subcarriers. The assumption of time-invariant frequency-selective multipath channels, ensures orthogonality between the subcarriers and thus, allows the use of a simple one-tap equalizer for recovering the transmitted symbol at each subcarrier.

In applications with high levels of mobility and rate, i.e., as in vehicular communications [9], the involved channels are usually time- and frequency- selective (so called doubly selective), and temporal variations within one OFDM block corrupt the orthogonality of different subcarriers, generating power leakage among them. This phenomenon makes the single-tap equalization unreliable [10, 11] since it is not able to mitigate the interference between the non orthogonal subcarriers (Intercarrier Interference ICI).

To deal with the issue of ICI, several approaches offering various complexity-performance tradeoffs have been proposed. Jeon et al. [12] truncated the channel matrix discarding a small number of coefficients, in order to reduce the dimension of matrix inversion for ZF equalizer. Choi et al. [13], presented linear and decision-feedback frequency domain equalizers. Cai and Giannakis [14], derived a low-complexity equalization scheme which was based on channel truncation and successive interference cancellation. This approach has also been exploited in [15, 16]. Schniter [17] derived an iterative equalizer which was composed by two stages, a first stage for ICI reduction and a second one for performing MMSE equalization. A standard approach used

This work was supported in part by EU and national funds via the National Strategic Reference Framework (NSRF) - Research Funding Program Thales (ENDECON), and in part by the University of Patras.

16th EANN workshops, September 25 - 28, 2015, Rhodes Island, Greece
© 2015 ACM. ISBN 978-1-4503-3580-5/15/09…$15.00
DOI: http://dx.doi.org/10.1145/2797143.2797152

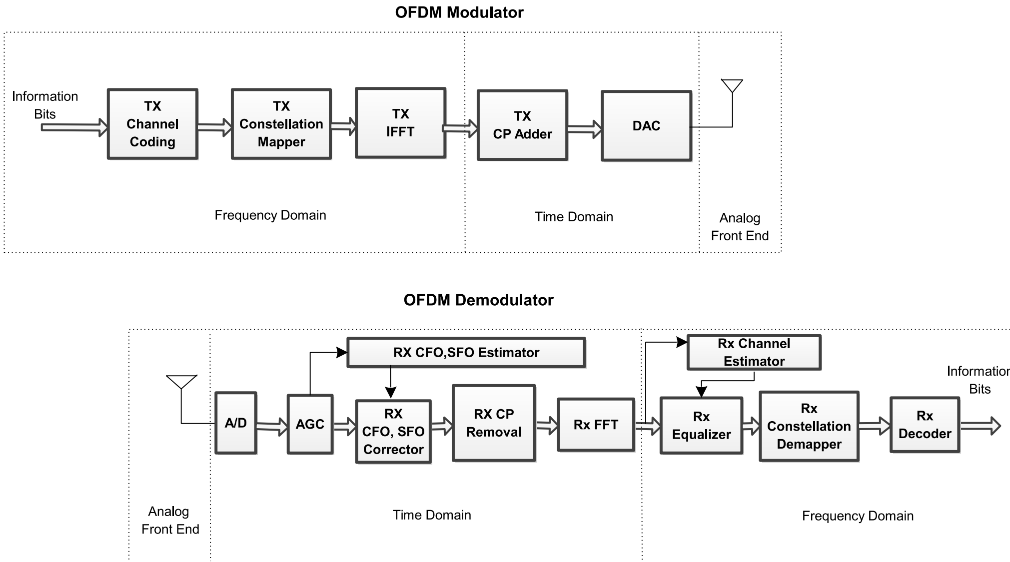

Figure 1: OFDM block diagram

for the design of low-complexity equalizers in all the aforementioned works, is the approximation of the channel matrix in the frequency-domain with a banded one. This operation corresponds to the mitigation of interference of only a small number of selected subcarriers that is determined by a truncation factor.

The aforementioned approximation leads, however, to reduction of both the computational complexity and equalization performance as well. In this paper we propose a regularization method for introducing additional information to the MMSE equalization design problem in order to minimize the performance degradation occured by matrix truncation. It is shown that by taking into account the frequency-domain correlation between different subcarriers we can significantly minimize the equalization performance degradation due to the use of the banded channel matrix, by achieving at the same time a quadratic complexity with respect to the number of the subcarriers. Finally, the proposed method is compared with several other methods of the related literature through extensive simulations, for very high mobile speeds, producing bit error rate and mean squared error curves for different channel impulse response lengths and sizes of the banded approximation (when applicable).

The rest of this paper is organized as follows. We present the system model in Section II, where the channel model and the OFDM system are briefly described. In Section III, MMSE ICI equalization schemes are reviewed, while in Section IV the new regularized scheme is derived. In Section V, the proposed algorithm's performance is evaluated through appropriate simulations. Finally, this paper is concluded in Section VI.

Notation: Lower-(upper-)case boldface letters are reserved for column vectors (matrices); the imaginary unit is denoted by $j = \sqrt{-1}$; $[A]_{i,j}$ denotes the component of the matrix $\mathbf{A}$ at the i-th row and the j-th column; $\delta(\cdot)$ denotes the Dirac's delta function; $(\cdot)^T, (\cdot)^H, (\cdot)^*$ denote the matrix transpose, complex conjugate transpose and complex conjugate respectively; $\mathcal{B}_Q(\mathbf{M})$ denotes the banded truncation of the matrix M, with $2Q+1$ non-zero elements at each row; $A_{|\Omega}$ denotes the submatrix with columns of $\mathbf{A}$ based on the index set Ω; $\mathbf{x}_{|\Omega}$ denotes the subvector with elements of $\mathbf{x}$ based on the index set Ω; $\mathbf{0}_{N\times N}$ denotes a $N \times N$ matrix with zeros and $\mathbf{I}_N$ the $N \times N$ identity matrix.

2. SYSTEM MODEL

Let us consider an OFDM system with N subcarriers operating over a time- and frequency-selective discrete-time baseband equivalent channel. A simplified block diagram of an OFDM transceiver, ignoring the units that perform Sampling Frequency estimation and Carrier Frequency Offset estimation and mitigation, is depicted in Fig. 1. Let $\mathbf{s} = [\begin{array}{ccc} s_1 & \dots & s_N \end{array}]^T$ be a set of N symbols at the output of the Constellation Mapper that are forwarded to the input of the Inverse Discrete Fourier Transform (IDFT) unit. The s_k symbol is transmitted via the k-th subcarrier. The output of the IDFT unit, denoted by $\mathbf{u} = \mathbf{F}^H\mathbf{s}$, is forwarded at the CP Adder, where the time domain OFDM symbol $\hat{\mathbf{u}}$ of length $M = N + N_{cp}$ is formed by adding a CP of length N_{cp} at the beginning of vector $\mathbf{s}$. This operation may be described in matrix form as follows

$$\hat{\mathbf{u}} = \mathbf{C}^{cp}\mathbf{u} = \left[\begin{array}{cc} \mathbf{0}_{(N-N_{cp})\times N} & \mathbf{I}_{N_{cp}} \\ \multicolumn{2}{c}{\mathbf{I}_N} \end{array}\right]\mathbf{u}. \quad (1)$$

In wireless communications, a doubly selective fading channel is often modeled as a Wide Sense Stationary Uncorrelated Scattering (WSSUS) channel [18]. In a discrete time model, the channel impulse response (CIR) of this WSSUS

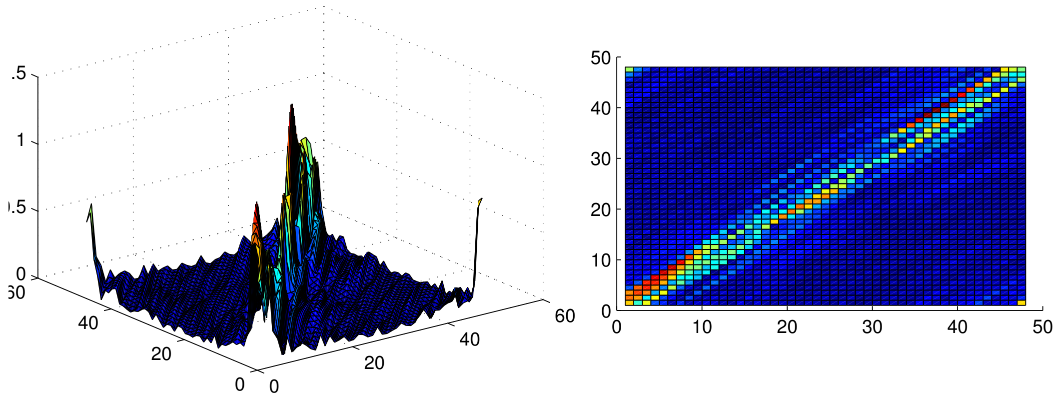

Figure 2: ICI power for doubly selective channel with 48 subcarriers and relative speed $v = 400$km/s in 3d (left figure) and 2d (right figure) plots.

channel can be expressed as

$$h(n,\tau) = \sum_{l=0}^{L-1} a(n,l)\delta(\tau - l) \qquad (2)$$

where $a(n,l)$ is complex zero mean Gaussian random variable. Assuming a causal channel with maximum delay spread $L \leq N_{cp}$, the received signal at the input of the OFDM demodulator may be written in matrix form as

$$\mathbf{x} \;=\; \tilde{\mathbf{H}}_t \hat{\mathbf{u}} + \hat{\mathbf{w}} \qquad (3)$$

where $[\tilde{H}_t]_{i,j} = a\left(i, (i-j) \mod N\right)$, and $\hat{\mathbf{w}}$ is a vector with complex Gaussian entries with zero mean and variance σ^2. If we ignore the sampling and carrier frequency offset, the block of time-domain samples $\mathbf{x}$, passes through the CP Removal unit of the OFDM demodulator, where the first N_{cp} samples are discarded. This operation may be written in matrix form as

$$\mathbf{z} = \mathbf{R}^{cp}\mathbf{x} = \left[\begin{array}{cc} \mathbf{0}_{(M-N)\times N} & \mathbf{I}_N \end{array}\right] \mathbf{x}. \qquad (4)$$

Then, vector $\mathbf{z}$ passes through the DFT unit whose output is given by:

$$\mathbf{y} = \mathbf{F}\mathbf{z} = \underbrace{\mathbf{F}\mathbf{R}^{cp}\tilde{\mathbf{H}}_t\mathbf{C}^{cp}\mathbf{F}^H}_{\mathbf{H}}\mathbf{s} + \mathbf{w} = \mathbf{H}\mathbf{s} + \mathbf{w} \qquad (5)$$

where, due to the unitary property of $\mathbf{F}$, the entries of $\mathbf{w}$ are complex Gaussian random variables with zero mean and variance σ^2.

If the involved channel is time-invariant, i.e. $a_i(1) = a_i(2) = \cdots = a_i(N)$, $i = 1, \ldots L$, the matrix $\mathbf{H}$ becomes diagonal since $\mathbf{R}^{cp}\tilde{\mathbf{H}}_t\mathbf{C}^{cp}$ has a circulant structure, and therefore equalization is possible with $\mathcal{O}(N)$ operations. On the contrary, in case the channel is time-varying which is the case of interest here, the matrix $\mathbf{H}$ is no longer diagonal (cf. Fig. 2) due to the introduced ICI, and, hence, nontrivial equalization techniques are required.

3. MMSE-BASED ICI SUPPRESION SCHEMES

The suppression of ICI in OFDM systems, transmitting through doubly-selective channels, can be achieved by various equalization approaches employing either linear or decision-feedback structures and applying different criteria for configuring the equalizer taps like Minimum Mean Squared Error (MMSE) and Least Squares (LS). Generally speaking, the performance of ICI mitigation is better for decision-feedback structures and MMSE-based criteria although the computational complexity is higher. In the following, we briefly review some well-known equalizers that can be utilized for the problem at hand focusing on the MMSE criterion. Their performance, as well as their computational complexity, will be compared, later on, with the proposed technique.

3.1 Block MMSE Equalizer

The MMSE equalizer for suppressing ICI in (5), assuming that $\mathbf{H}$ is known and that $\mathbf{s}$ and $\mathbf{w}$ are uncorrelated to each other, is given by

$$\tilde{\mathbf{s}} = \mathbf{G}^H\mathbf{y} = \mathbf{R}^{-1}\mathbf{H}\mathbf{y}, \qquad (6)$$

where

$$\mathbf{R} \triangleq E\{\mathbf{y}\mathbf{y}^H\} = \mathbf{H}\mathbf{H}^H + \sigma_w^2\mathbf{I}_N.$$

The computational cost in order to solve (6) requires $\mathcal{O}(N^3)$ operations, in the general case.

3.2 Banded MMSE Equalizer

The block MMSE equalizer, presented in the previous section, is considered to have high computational complexity especially in the cases of a large number of subcarriers (employed by OFDM) and/or of time-varying channels as in vehicular communications (requiring frequent recalculation of the equalizer taps).

Among others, in [12], it was mentioned that ICI is mainly evident in neighboring subcarriers, meaning that the channel matrix $\mathbf{H}$ has a strongly banded form as depicted in Fig. 2. In order to reduce the complexity, it was proposed that instead of using the full channel matrix $\mathbf{H}$, a banded version is used, namely $\hat{\mathbf{H}} = \mathcal{B}_Q(\mathbf{H})$, where $\mathcal{B}_Q(\cdot)$ denotes the operation of keeping $K = 2Q + 1$ diagonals of the matrix $\mathbf{H}$ centered around the main diagonal. The size of K

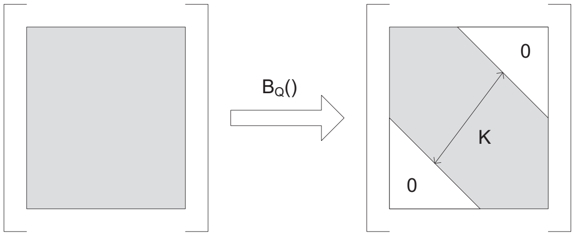

Figure 3: The $\mathcal{B}_Q(\cdot)$ operation. Transforming a matrix to a banded one of bandwidth K.

depends on the maximum Doppler spread f_d and should be increased for large f_d's, i.e for fast time varying channels. Fig. 3 depicts this operation. The MMSE equalizer in this case is similar to the one in (6) where the banded matrix $\hat{\mathbf{H}}$ is used instead of $\mathbf{H}$. The computational complexity of this equalizer is $\mathcal{O}(NK^2)$ operations when the special structure of the channel matrix is taken into account. As it is understood, the less K is, the lower the computation complexity is. However, this has a negative effect on performance.

3.3 Serial MMSE Equalizer

The banded MMSE equalizer has reduced computational complexity when compared with the block MMSE equalizer, however for small values of K, i.e. for slowly time varying channels. Also, it has worse performance than the block MMSE equalizer. In [14], an iterative equalizer was proposed with the aim to improve the performance of the banded equalizer and at the same time keep the complexity lower than the block MMSE equalizer. This was achieved by utilizing recursions over the subcarriers during the operation of the equalizer.

Specifically, for each subcarrier k, a sub-vector of $\mathbf{y}$ is retained by carefully selecting K elements (in a rotating manner). In this way, the inverse of the autocorrelation matrix used in the k-th subcarrier can be calculated recursively by the corresponding matrix of the $k-1$-th subcarrier leading to a complexity of $\mathcal{O}(NK)$ per subcarrier iteration and to $\mathcal{O}(N^2K)$ for the whole OFDM block.

3.4 Successive Interference Cancellation

Successive interference cancellation (SIC) may offer a more effective ICI reduction as compared to linear equalization with the cost of higher complexity [13]. To comprehend the basic idea, let us first recall that each subcarrier is related with one of the N transmitted data symbols. Thus, SIC architecture is comprised by N stages, where at each stage we can easily subtract the part of the ICI which is associated with the decisions already made at previous stages.

Specifically, let us consider that the symbols are detected successively in the order $s_{z_1}, s_{z_2}, \ldots, s_{z_N}$. Then at the z_k-th stage, we seek for the minimizer of the cost function

$$\mathbf{g}_{z_k} = arg\min_{\mathbf{g}_{z_k}} \mathcal{E}\{\|\mathbf{g}_{z_k}^T \mathbf{y}_{z_k} - s_{z_k}\|_2^2\} \tag{7}$$

where $\mathbf{g}_{z_k}$ denotes the equalizer filter of the z_k stage, and $\mathbf{y}_{z_k}$ is the updated vector of the received OFDM block after cancelling the $k-1$ previously detected symbols. Equivalently, it is given as the solution of the following system of equations

$$\mathbf{R}_{z_k}\mathbf{g}_{z_k}^T = \mathbf{h}_{z_k}^H \tag{8}$$

Table 1: Successive Interference Cancellation Algorithm

Inputs: $\mathbf{R}, \mathbf{H}, [z_1, z_2, \ldots, z_N]$
Repeat for all stages z_k :
Step 1: Solve the system $\mathbf{R}_{z_k}\mathbf{g}_{z_k}^H = \mathbf{h}_{z_k}^H$, to compute the equalizer vector $\mathbf{g}_{z_k}$ for the z_k-th subcarrier symbol.
Step 2: Estimate the z_k-th subcarrier symbol, $\tilde{s}_{z_k} = \mathbf{g}_{z_k}^H \mathbf{y}$.
Step 3: Detect the z_k-th subcarrier symbol, $\hat{s}_{z_k} = \Pi(\tilde{s}_{z_k})$.
Step 4: Cancel the z_k-th symbol ICI from $\mathbf{y}_{z_k}$, $\mathbf{y}_{z_{k+1}} = \mathbf{y}_{z_k} - \mathbf{h}_{z_k}\hat{s}_{z_k}$.
Step 5: Update the autocorrelation matrix, $\mathbf{R}_{z_{k+1}} = \mathbf{H}_{z_k}^H \mathbf{H}_{z_k} + \sigma^2 \mathbf{I}_{N-k}$.

where $\mathbf{h}_{z_k}$ is the z_k-th column of the channel matrix $\mathbf{H}$. If $\mathbf{H}_{z_k}$ denotes the channel matrix after the removal of z_k column, then the autocorrelation matrix of the next stage z_{k+1} is computed according to

$$\mathbf{R}_{z_{k+1}} = \mathbf{H}_{z_k}^H \mathbf{H}_{z_k} + \sigma^2 \mathbf{I}_{N-k} \tag{9}$$

given that $\mathbf{H}_{z_1} \triangleq \mathbf{H}$. Note that, at each subsequent stage, the size of the autocorrelation matrix $\mathbf{R}_{z_{k+1}}$ is reduced by one.

The detection of the current symbol is expressed as $\hat{s}_{z_k} = \Pi(\mathbf{g}_{z_k}^H \mathbf{y})$, where $\mathbf{g}_{z_k}^T = \mathbf{h}_{z_k}^H \mathbf{R}_{z_k}^{-1}$. The symbol decision $\hat{s}_{z_k}$ is used to provide an estimate of the respective ICI, that is $\mathbf{h}_{z_k}\hat{s}_{z_k}$, which in the next iteration z_{k+1}, it will be subtracted from the received OFDM block, i.e.

$$\mathbf{y}_{z_{k+1}} = \mathbf{y}_{z_k} - \mathbf{h}_{z_k}\hat{s}_{z_k} \tag{10}$$

given that $\mathbf{y}_{z_1} \triangleq \mathbf{y}$, and the procedure continues likewise for the next subcarrier symbol $s_{z_{k+1}}$. The resulting SIC architecture is summarized at Table 1.

Since this architecture resembles that of a decision feedback equalizer [19], one can expect an error propagation phenomenon. However, assuming that $\hat{s}_{z_k}$ has been correctly detected, its interference will be canceled from the subsequent stages.

It is well-known that the detection order in SIC architecture has significant impact on the performance of the equalizer [20, 19]. Typically, the optimal detection order can be obtained by maximizing the signal-to-interference and noise power ratio (SINR) at the receiver, since it is known that the maximization of the SINR also minimizes the achievable bit error rate (BER) in an OFDM system [21]. Hence, at each stage k, we have that

$$\mathrm{SINR}_k = \frac{|\mathbf{g}_k^H \mathbf{h}_k|^2}{\sum_{m,m\neq k} |\mathbf{g}_k^H \mathbf{h}_m|^2 + \sigma\|\mathbf{g}_k\|_2^2}, \quad \forall k \in [z_{k+1}, \ldots, z_N]. \tag{11}$$

Note that, the computation of SINR_k at stage z_k, requires the knowledge of $\mathbf{g}_{z_{k+1}}, \ldots, \mathbf{g}_{z_N}$ equalization vectors, which are obtained from the solution of the following systems

$$\mathbf{R}_{z_k}\mathbf{g}_{z_l}^T = \mathbf{h}_{z_l}^H, \text{ with } l \in [k+1, N]. \tag{12}$$

The autocorrelation matrix in Eq. (12) is the same for all the RHS, since it is updated once per stage. Equivalently, concatenating the equalization vectors of the current stage

z_k and the subsequent stages $z_{k+1}, \ldots, z_N$, into the matrix $\mathbf{G}_{z_k} = [\mathbf{g}_{z_k} \mathbf{g}_{z_{k+1}} \ldots \mathbf{g}_{z_N}]^T \in \mathbb{C}^{N-k \times N}$, the equalization matrix for the current stage is obtained by the solution of the following system of equations with N RHS,

$$\mathbf{R}_{z_k} \mathbf{G}_{z_k} = \mathbf{H}_{z_k}^H. \tag{13}$$

Therefore, the complexity burden of the scheme is dominated by the complexity of Step 1, that is, the solution of the system (13) for all N stages. A solution through a direct approach would require $\mathcal{O}(N^3)$ complexity.

4. PROPOSED METHOD

4.1 Regularized Equalizer

As it has been described in the previous Section, in order to reduce the complexity of the ICI equalization, we consider a banded part of the channel matrix A, with only K terms at each row, neglecting the $N-K$ remaining ones. In order to reduce the truncation effects to the MSE between the original and recovered signal, a regularized estimation has been proposed in [22]. This technique exploits the statistics of the error term, aiming to improve the performance of the banded block linear MMSE equalizer, retaining the same complexity cost.

Let the received symbols in the frequency-domain be expressed as

$$\mathbf{y} = \underbrace{\hat{\mathbf{A}}\mathbf{s}}_{\text{signal}} + \underbrace{\boldsymbol{\Delta}\mathbf{s} + \mathbf{w}}_{\text{noise term}} \tag{14}$$

where the AGWN and the model-error $\boldsymbol{\Delta}\mathbf{s}$ have been grouped together as the noise term.

By using Eq. (14) in (6), the block MMSE estimator is expressed as

$$E\left\{\left[(\hat{\mathbf{A}} + \boldsymbol{\Delta})\mathbf{s} + \mathbf{w}\right]\left[(\hat{\mathbf{A}} + \boldsymbol{\Delta})\mathbf{s} + \mathbf{w}\right]^H\right\}\mathbf{G} = \tag{15}$$

$$E\left\{\left[(\hat{\mathbf{A}} + \boldsymbol{\Delta})\mathbf{s} + \mathbf{w}\right]\mathbf{s}^H\right\} \tag{16}$$

$$\Rightarrow (\hat{\mathbf{A}}\hat{\mathbf{A}}^H + \sigma_w^2 \mathbf{I} + E\{\boldsymbol{\Delta}\boldsymbol{\Delta}^H\})\mathbf{G} = \hat{\mathbf{A}} \tag{17}$$

where $\mathbf{G}$ is actually a regularized estimator. Under proper conditions [22], the matrix $E\{\boldsymbol{\Delta}\boldsymbol{\Delta}^H\}$ can be approximated by a banded one, i.e.

$$E\{\boldsymbol{\Delta}\boldsymbol{\Delta}^H\} \simeq \mathcal{B}(E\{\boldsymbol{\Delta}\boldsymbol{\Delta}^H\}) \equiv \mathbf{B}\mathbf{B}^H. \tag{18}$$

In that case, Eq. (17) can be expressed as

$$(\hat{\mathbf{A}}\hat{\mathbf{A}}^H + \sigma_w^2 \mathbf{I} + \mathbf{B}\mathbf{B}^H)\mathbf{G}_b = \hat{\mathbf{A}} \tag{19}$$

Since $\mathbf{R} \triangleq \hat{\mathbf{A}}\hat{\mathbf{A}}^H + \sigma_w^2 \mathbf{I} + \mathbf{B}\mathbf{B}^H$ is a Hermitian band matrix, the solution of (19) can be obtained through the low-complexity banded $\mathbf{LDL}^H$ factorization [23], [22].

4.2 Regularized SIC

In this section, we extend the described regularization framework to the SIC case. A straightforward approach would be the deployment of LDL decomposition at each successive stage. However, this would imply complexity of the order $\mathcal{O}(N^2K^2)$. Indeed, at each stage, the banded matrix $\mathbf{R}_k$ has to be computed via a rank-one update, i.e.

$$\mathbf{R}_\mathbf{k} = \mathbf{R}_{k-1} - \hat{\mathbf{A}}_{k-1}\hat{\mathbf{A}}_{k-1}^H \tag{20}$$

Table 2: Proposed Algorithm

Inputs: $\hat{\mathbf{A}}, [z_1, z_2, \ldots, z_N]$
Construct the banded matrix $\mathbf{R}_1$
Perform banded $\mathbf{LDL}^H$ factorization
Compute the equalization matrix
$\mathbf{g}_1 = (\mathbf{L}^H)^{-1}\left[\mathbf{D}^{-1}\left(\mathbf{L}^{-1}\hat{\mathbf{A}}_1\right)\right]$
Repeat for all stages $k = 1, \ldots, N$:
Estimate the k-th subcarrier symbol,
$\tilde{s}_k = \mathbf{g}_k^H \mathbf{y}$.
Detect the k-th subcarrier symbol,
$\hat{s}_k = \Pi(\tilde{s}_k)$.
Cancel the k-th symbol ICI from $\mathbf{y}_k$,
$\mathbf{y}_{k+1} = \mathbf{y}_k - \mathbf{h}_k \hat{s}_k$
Update the inverse matrix
$\mathbf{R}_{k+1}^{-1} = \mathbf{R}_k^{-1} - \frac{\mathbf{R}_k^{-1}\hat{\mathbf{A}}_k\hat{\mathbf{A}}_k^H\mathbf{R}_k^{-1}}{1+\hat{\mathbf{A}}_k^H\mathbf{R}_k^{-1}\hat{\mathbf{A}}_k}$
Solve the system via inversion lemma
$\mathbf{g}_{k+1} = \mathbf{R}_{k+1}^{-1}\hat{\mathbf{A}}_{k+1}$

Table 3: Complexity Order Comparisons

Equalizer	Complexity
block non-banded OSIC [13]	$\mathcal{O}(N^4)$
block non-banded linear	$\mathcal{O}(N^3)$
serial DFE [14]	$\mathcal{O}(N^2K)$
block banded SIC [24]	$\mathcal{O}(NK^2)$
block banded reg. SIC (prop.)	$\mathcal{O}(N^2K)$
block banded regularized linear [22]	$\mathcal{O}(NK^2)$

with $\mathbf{R}_0 = \hat{\mathbf{A}}\hat{\mathbf{A}}^H + \sigma_w^2 \mathbf{I} + \mathbf{B}\mathbf{B}^H$, and the k-stage equalizer vector is given by the solution of the system

$$\mathbf{R}_k \mathbf{g}_k = \hat{\mathbf{A}}_k \tag{21}$$

The LDL method may solve this system with cost equal to $\mathcal{O}(NK^2)$.

In order to reduce the involved complexity, we employ the inversion lemma to compute the inverse of the matrix, i.e.

$$\mathbf{R}_{k+1}^{-1} = \left(\mathbf{R}_k - \hat{\mathbf{A}}_k\hat{\mathbf{A}}_k^H\right)^{-1} \tag{22}$$

$$= \mathbf{R}_k^{-1} - \frac{\mathbf{R}_k^{-1}\hat{\mathbf{A}}_k\hat{\mathbf{A}}_k^H\mathbf{R}_k^{-1}}{1 - \hat{\mathbf{A}}_k^H\mathbf{R}_k^{-1}\hat{\mathbf{A}}_k} \tag{23}$$

This reduces the computational cost of each stage to $\mathcal{O}(NK)$, since only matrix-vector computations are required. The overall equalization method is summarized in the Table 2.

Since all the involved matrices are banded, with K off-diagonal elements for each row, the computational complexity order of the algorithm is $\mathcal{O}(N^2K)$. In Table 3, we compare the complexities of some representive equalization schemes, from the non-banded, banded and serial classes.

5. SIMULATION RESULTS

In this section, we provide some indicative simulation results in order to evaluate the performance of the proposed method. We consider an OFDM communication system operating over a doubly selective channel, with parameters drawn from the IEEE 802.11p standard [9]. According to this standard, the number of the subcarriers is 64 but only the inner 48 subcarriers contain data; Table 4 summarizes

Table 4: Basic parameters for 802.11p standard

Parameter	Value
Bit rate (Mb/s)	3, 4.5, 6, 9, 12, 18, 24, 27
Modulation mode	BPSK, QPSK, 16-64 QAM
Code rate	1/2, 2/3, 3/4
Number of subcarriers	52
Symbol duration	8 μs
Guard time	1.6 μs
FFT period	6.4 μs

Table 5: Normalized maximum Doppler shift for 802.11p standard

	Channel spacing		
v_{max} (km/h)	20 MHz	10 MHz	5 MHz
100	0.0021	0.0042	0.0083
200	0.0042	0.0083	0.0166
300	0.0062	0.0125	0.0249
400	0.0083	0.0166	0.0333

some of the basic parameters of 802.11p standard. Table 5 lists the normalized maximum Doppler shift f_d with respect to the channel spacing and the vehicle-to-vehicle relative speed.

We adopt a Rayleigh wide sense stationary (WSSUS) channel model with exponential decaying power delay profile (PDP),

$$\text{PDP}(l) = \frac{e^{-l}/L}{\sum_{i=1}^{L} e^{-l}}, l = 1, \dots, L. \quad (24)$$

The channel spacing is assumed to be at 5 MHz, while the carrier frequency is $f_C = 5.8$ GHz. Furthermore, we assume a maximum relative velocity between the transmitter and the receiver of $v_{max} = 400$ km/h, and that the OFDM symbol duration is set to $T_S = 16\mu$s (i.e. 64 subcarriers), hence in this case the maximum normalized Doppler frequency is given by $f_d = \frac{v_{max}}{c_0} f_C T_S = 0.0333$.

To evaluate the performance of the proposed equalizer, we have employed techniques which belong to the classes of non-banded, banded and serial equalizers. Specifically, from the class of non-banded methods we employ the block OSIC MMSE equalizer [13], while from the class of serial methods the equalizer of [14]. The former technique achieves a very good performance at the expense of a very high complexity cost, i.e. $\mathcal{O}(N^4)$. On the other hand, banded and serial MMSE equalizers reduce the equalization cost along with the performance. In our simulation results, we employ the following methods from the banded class: the block banded linear MMSE equalizer [12], the block banded regularized linear MMSE equalizer [22], and the block banded regularized SIC MMSE equalizer (proposed). Also note that all the banded equalizers have a band equal to $K = 2D + 1$, while the serial one has window length also equal to K.

In Fig. 4, we evaluate the performance of the proposed equalizer in terms of bit error rate (BER) w.r.t. SNR, while in Fig. 5 the respective mean square error (MSE) w.r.t SNR. The channel length in this case was set to $L = 3$ while we have used 4-QAM modulation. The linear techniques (drawn with dashed lines) have the worst performance, with their an increase to their BER w.r.t. the SNR. This is caused due to the ill condition of the banded chan-

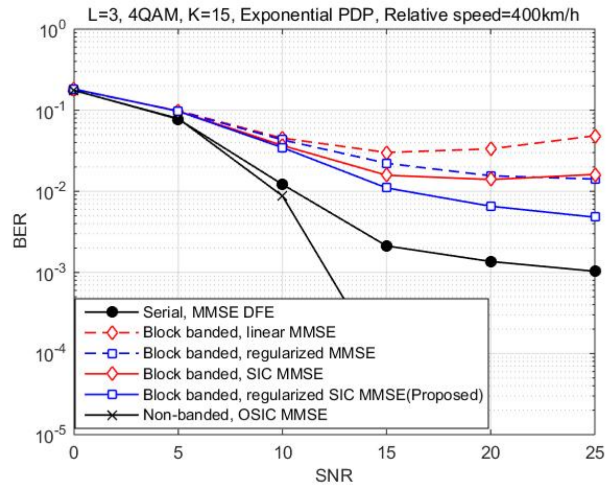

Figure 4: Comparison of BER versus SNR for channel length $L = 3$

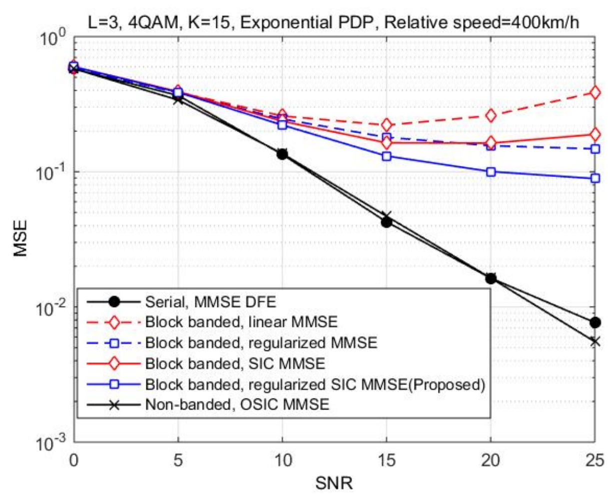

Figure 5: Comparison of MSE versus SNR for channel length $L = 3$.

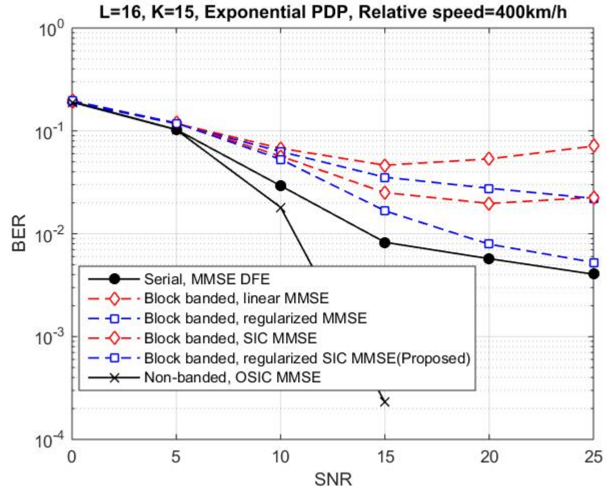

Figure 6: Comparison of BER versus SNR for channel length $L = 16$.

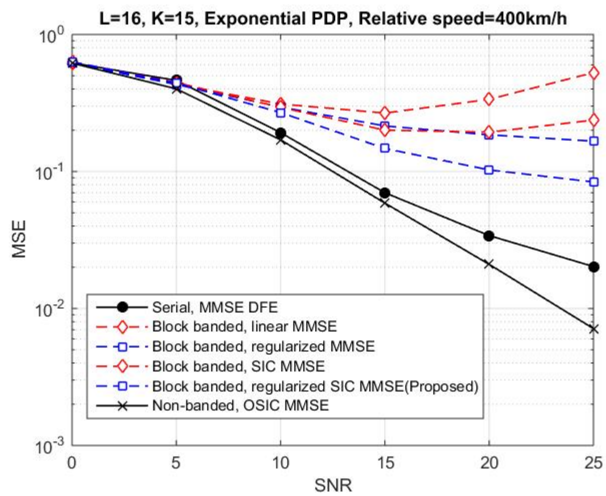

Figure 7: Comparison of MSE versus SNR for channel length $L = 3$.

nel matrix. The lower BER performance was exhibited by the non-banded OSIC scheme. Furthermore, the regularized techniques (drawn with solid blue lines) seem to improve the performance of the banded equalizers, for both cases of the linear and the cancellation schemes.

In Figs. 6-7 the BER and MSE performance curves are shown for the case where the channel has long temporal span, i.e. $L = 16$. From these Figures it can be deduced that the serial DFE technique is heavily affected, exhibiting worse performance than the previous channel length case. However, the proposed technique seems to be unaffected with the channel length, along with the other banded and non-banded ones.

In Fig. 8, we show the BER performance w.r.t. the length of the band/window K. The comparison was conducted at a fixed SNR of $15dB$. The performance of all approximated schemes increases w.r.t K, however the regularized schemes seem to be significantly favored with the increase of K.

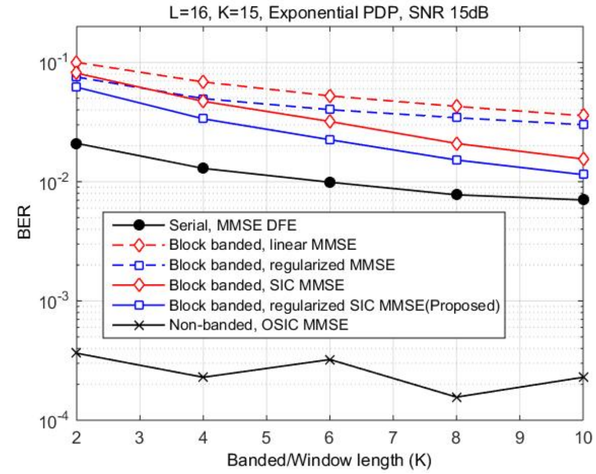

Figure 8: Comparison of BER versus the length of the banded/widowed approximation

6. CONCLUSION

In V2V commnunication systems, the wireless channel is characterized by double selectivity, and thus intercarrier interference (ICI) is introduced at the receiver. Equalization is usually employed to mitigate this effect, adopting usually a banded approximation for the frequency domain matrix, in order to reduce the complexity cost. We have shown that this approximation degrades significantly the performance of the V2V system, and we have proposed a regularized successive interference cancellation scheme. Through extensive simulations we have verified that this scheme recovers this performance loss, while the complexity remains quadratic to the number of the subcarriers.

7. REFERENCES

[1] J. G. Andrews et al. What will 5g be? *IEEE Journal on Selected Areas in Communications*, 32(6):1065 – 1082, Jun. 2014.

[2] ETSI. Digital audio broadcasting (dab) to mobile, portable and fixed receivers. *ETS*, 300 401, 1995.

[3] ETSI. Digital video broadcasting (dvb): Transmission system for hand-held terminals (dvb-h). *ETSI*, EN 302 304 V1.1.1, Nov. 2004.

[4] IEEE P802 LAN/MAN Committee. The working group on broadband wireless access standards.

[5] Agillent Technologies. 3GPP Long Term Evolution: System Overview, Product development and Test challenges. Application note, iterature number 5989-8139EN, May 19,2008.

[6] G. Baldini, S. Karanasios, D. Allen, and F. Vergari. Survey of wireless communication technologies for public safety. *IEEE Communications Surveys and Tutorials*, 16(2):619 – 641, Q2 2014.

[7] G. Karagiannis, O. Altintas, E. Ekici, G. Heijenk, B. Jarupan, K. Lin, and T. Weil. Vehicular networking: A survey and tutorial on requirements, architectures, challenges, standards and solutions. *IEEE Communications Surveys and Tutorials*, 13(4):584 – 616, Jul. 2011.

[8] E. Uhlemann. Introducing connected vehicles. *IEEE Vehicular Technology Magazine*, 10(1):23 – 31, Mar. 2015.

[9] Part 11: Wireless LAN medium access control (MAC) and physical layer (PHY) specifications amendment 6: Wireless access in vehicular environments. *IEEE 802.11p published standard*, Jul. 2011.

[10] Tiejun Wang, J.G. Proakis, E. Masry, and J.R. Zeidler. Performance degradation of ofdm systems due to doppler spreading. *IEEE Transactions on Wireless Communications*, 5(6):1422 – 1432, Jun. 2006.

[11] P. Robertson and S. Kaiser. The effects of doppler spreads in ofdm(a) mobile radio systems. In *Vehicular Technology Conference*, volume 1, pages 329 – 333, 1999.

[12] Won Gi Jeon, Kyung Hi Chang, and Yong Soo Cho. An equalization technique for orthogonal frequency-division multiplexing systems in time-variant multipath channels. *IEEE Transactions on Communications*, 47(1):27 –32, Jan. 1999.

[13] Y. S. Choi, P. J. Voltz, and F. A. Cassara. On channel estimation and detection for multicarrier signals in fast and selective rayleigh fading channels. *IEEE Transactions on Communications*, 49(8):1375 – 1387, 2001.

[14] Xiaodong Cai and G.B. Giannakis. Bounding performance and suppressing intercarrier interference in wireless mobile ofdm. *IEEE Transactions on Communications*, 51(12):2047 – 2056, Dec. 2003.

[15] S. U. Hwang, H. Jeong Lee, and J. Seo. Low complexity iterative ici cancellation and equalization for ofdm systems over doubly selective channels. *IEEE Transactions on Broadcasting*, 55(1):132 –139, march 2009.

[16] G. Taubock, M. Hampejs, P. Svac, G. Matz, F. Hlawatsch, and K. Grochenig. Low-complexity ici/isi equalization in doubly dispersive multicarrier systems using a decision-feedback lsqr algorithm. *IEEE Transactions on Signal Processing*, 59(5):2432 –2436, may 2011.

[17] P. Schniter. Low-complexity equalization of ofdm in doubly selective channels. *IEEE Transactions on Signal Processing*, 52(4):1002 – 1011, Apr. 2004.

[18] P. Bello. Characterization of randomly time-variant linear channels. *IEEE Transactions on Communications Systems*, 11(4):360 – 393, Dec. 1963.

[19] A. Lozano and C. Papadias. Layered space-time receivers for frequency-selective wireless channels. *IEEE Transactions on Communications*, 50(1):65–73, Jan. 2002.

[20] P. W. Wolniansky, G. J. Foschini, G. D. Golden, and R. A. Valenzuela. V-BLAST: An architecture for realizing very high data rates over the rich-scattering wireless channel. *Bell Laboratories, Lucent Technologies, Crawford Hill Laboratory.*

[21] S.N. Diggavi. Analysis of multicarrier transmission in time-varying channels. In *IEEE International Conference on Communications, 1997. ICC '97*, volume 3, pages 1191– 1195, Jun. 1997.

[22] E. Vlachos, A.S. Lalos, and K. Berberidis. Regularized MMSE ICI equalization for OFDM systems over doubly selective channels. In *2013 IEEE International Symposium on Signal Processing and Information Technology (ISSPIT)*, pages 458–463, Dec. 2013.

[23] Luca Rugini, Paolo Banelli, and Geert Leus. Simple equalization of time-varying channels for ofdm. *IEEE Communications Letters*, 9(7):619–621, 2005.

[24] Luca Rugini, Paolo Banelli, and Geert Leus. Low-complexity banded equalizers for ofdm systems in doppler spread channels. *EURASIP J. Appl. Signal Process.*, 2006:248–248, January 2006.